Comparative Studies of Cation Doping of ZnO with Mn, Fe, and Co[†]

Karl Jug* and Viatcheslav A. Tikhomirov[‡]

Theoretische Chemie, Leibniz Universität Hannover, Callinstr. 3A, 30167 Hannover, Germany

Received: March 20, 2009; Revised Manuscript Received: July 22, 2009

MSINDO calculations were performed to elucidate the effect of doping and defects on the electronic properties of zinc oxide. The cyclic cluster $Zn_{48}O_{48}$ served as a model for the bulk. Band gaps and stabilities of spin states were determined for doping with Mn, Fe, and Co. It was found that a substantial lowering of the band gap occurs for Mn and Co doping. In contrast, the Fe doping has a rather insignificant effect on the band gap. Additional defects such as oxygen vacancy, zinc interstitial, or zinc vacancy were also studied. In the case of substitution of zinc by two transition metal atoms, various spin states arise which can be classified as antiferromagnetic, ferrimagnetic, or ferromagnetic. We find that the spin state with the lowest multiplicity, antiferromagentic or ferrimagnetic, is more stable than the high-multiplicity ferromagnetic state in most considered cases, but additional zinc vacancies or mixed doping may reverse this trend.

1. Introduction

The importance of ZnO for technological applications has been repeatedly emphasized in the past decade. The design of optoelectronic devices has been a major driving force.[1] Modification of the ZnO properties by impurity incorporation is currently debated in the context of possible applications in ultraviolet optoelectronics and spin electronics.[2,3] A representative review[4] gives a comprehensive picture of the knowledge on this compound with respect to properties such as crystal structure, lattice parameters, electronic band structure, mechanical properties, lattice dynamics, and thermal properties. Special attention is given to optical properties and how they are influenced by defects and doping. The understanding of the influence of defects and doping on the band gap is a challenging task, and the band gap engineering offers a great potential for optical applications. Beyond this, the doping of ZnO with transition metals can lead to magnetic semiconductors.

Recently, zinc-rich $Zn_{1-x}Mn_xO$ mixed crystals received considerable attention for possible diluted magnetic semiconductor (DMS) material for spintronics.[4,5] However, there is a controversy about the magnetism of $Zn_{1-x}Mn_xO$ at room temperature. One group[6] claimed ferromagnetism above room temperature in bulk and transparent films of Mn-doped ZnO, based on experimental and theoretical studies. Ferromagnetic ordering was found at Curie temperatures of $T_c > 420$ K in samples sintered below 700 °C. However, sintering above 700 °C suppressed the ferromagnetism to below room temperature. The same group used density functional theory (DFT) calculations to confirm ferromagnetism. The model assumes Zn substitution by Mn up to 4%. Others supported this idea but explained ferromagnetism by the presence of oxide phases,[7,8] defects in ZnO,[9,10] or simply by substitutional effects due to Mn substitution for Zn in the wurtzite phase[11] of thick Mn/Zn multilayers. In an investigation of Mn-doped ZnO pellets with diluted Mn concentration, Bondino et al.[12] found ferromagnetism for $Zn_{0.98}Mn_{0.02}O$ and no magnetic order for $Zn_{0.96}Mn_{0.04}O$.

In contrast, Tiwari et al.[13] found paramagnetic behavior with SQUID measurements in diluted semiconducting $Zn_{1-x}Mn_xO$ films. Fukumura et al.[5] ascribed the magnetization to a strong antiferromagnetic exchange coupling. Kolesnik et al.[14] found paramagnetic behavior with antiferromagnetic interactions in single-phase materials. Kolesnik and Dabrowski[15] then postulated the absence of room temperature ferromagnetism in bulk Mn-doped ZnO. They argued that a single phase $Zn_{1-x}Mn_xO$ ($x = 0.05$) can be synthesized in air only at temperatures above 900 °C. Chikoidze et al.[16] performed SQUID measurements between 5 and 300 K on thin $Zn_{1-x}Mn_xO$ films and found paramagnetic-like behavior for $x > 0.02$ with antiferromagnetic coupling. Density functional theory (DFT) calculations based on local spin density approximation (LSDA) and generalized gradient approximation[17] or pseudopotentials with localized atomic orbital basis sets[18] on $Zn_{1-x}Mn_xO$ resulted in the prediction of a slightly more energetically favorable antiferromagnetic state for pure $Zn_{1-x}Mn_xO$. Furthermore, defects such as Zn interstititals, oxygen vacancies, N-doping, and zinc vacancies in $Zn_{1-x}Mn_xO$ were studied by computation[5] and experiment.[19] Absence of ferromagnetism was also found by X-ray diffraction.[20]

Several of these groups also studied the electronic absorption spectra of $Zn_{1-x}Mn_xO$. Experimental[5,13,16] and theoretical[17] results predicted an increase of the band gap with increasing Mn content.

The same controversy applies to ZnO samples doped with other transition metals such as Fe or Co. Ferromagnetism was claimed by several groups,[22,23] whereas others argue in favor of antiferromagnetism.[21] One explanation was that there is no intrinsic ferromagnetism, but it resulted from the formation of doping transition metal oxide grains[22] or transition metal microclusters.[23] DFT calculations by Spaldin[24] and Ghopal and Spaldin[25] support antiferromagnetism or paramagnetism. Still newer experiments claim intrinsic ferromagetism in Fe-doped ZnO and discard the explanations of oxide grain and microclusters.[26] Another study found antiferromagnetism for 5% Fe doping but ferromagnetism for 10% Fe doping.[27] In contrast, X-ray absorption fine structure measurements give evidence of substitutional Co ion clusters in ZnO, which influence the magnetic properties.[28] Co clustering in ZnO was studied by

[†] Part of the "Walter Thiel Festschrift".

[‡] Permanent address: Karpov Institute of Physical Chemistry, ul. Vorontsovo Pole 10, Moscow 105064, Russia.

10.1021/jp902532a CCC: $40.75
Published on Web 08/20/2009

Sanyal et al.[29] in Monte Carlo simulations. The authors argued that in the case of 30% Co doping the Co atoms are close to each other and give rise to the formation of a metallic Co in a big spanning cluster with strong ferromagnetic interactions. This would explain qualitatively the wide variation of results on the ordering temperatures in experiments. In a more refined DFT electronic structure calculation on Co clustering in ZnO, Iuşan et al.[30] emphasized the importance of short-ranged antiferromagnetic interactions.

The goal of this paper is to focus on band gaps and magnetic properties such as antiferromagnetism, ferrimagnetism, and ferromagnetism. We have studied the cation doping of ZnO with Mn, Fe, and Co and its effect on the band gap and with Mn, Fe, and Co on the relative stabilities of the various spin arrangements. In the following sections, we describe the methods and models and show how the nuclear and electronic structure and the stability of ZnO are influenced by this doping.

2. Methods and Models

All quantum chemical calculations presented in this work were performed with MSINDO,[31,32] a semiempirical MO method with a documented accuracy for structure and energy, which was extended to third-row transition metal elements.[33] For solid state studies, the cyclic cluster model (CCM) was used. The method was designed to preserve the equivalence of atoms in an infinite system also in a cluster. This was achieved by creating equal environments for equivalent atoms by proper translation of the atoms. The CCM[34] was incorporated in MSINDO in order to achieve the effect of periodicity of a perfect crystalline solid in a finite cluster. For ionic systems, it is important to include long-range Coulombic effects. To achieve this goal, the cyclic cluster was embedded in an infinite field of point charges[35] using the Ewald summation technique. The cluster shape and size were measured by the relative average coordination number k.[36] This number is 1 for the infinite three-dimensional periodic crystal and less than 1 for free clusters. The coordination number of each atom is determined by the number of nearest neighbors. Then, the average coordination number of all atoms in the free cluster is calculated and divided by the average coordination number in the bulk. This number is kept also for the corresponding cyclic cluster for consistency reasons. The band gap was approximated as the difference between the energies of the lowest unoccupied molecular orbital (LUMO) and the highest occupied molecular orbital (HOMO). The LUMO was calculated by the improved virtual orbital (IVO) method.[37]

3. Doping and Defects in ZnO

3.1. Doping of ZnO with Mn. Zinc oxide has a hexagonal structure where each oxygen atom is bound to four zinc atoms and vice versa. The local arrangement is tetrahedral for each atom. We have chosen the cyclic cluster $Zn_{48}O_{48}$ as the starting point for our investigations. As we have previously[38] shown, this size is sufficient for studies of bulk defects and doping, because its heat of formation is converged within 0.1 kJ/mol. The calculated heat of atomization is 727.5 kJ/mol[39] compared to the experimental value of 728 kJ/mol,[40] and the calculated band gap of ZnO for this cluster size is 3.40 eV[38] compared to the experimental value of 3.44 eV at 0 K.[41]

Mixed phases of ZnO and MnO can be prepared by chemical vapor transport at about 950 °C with a maximum solubility of 20 mol % MnO in ZnO.[42] We calculated the substitution of one and two Zn atoms by Mn atoms in the cyclic cluster $Zn_{48}O_{48}$. This corresponds to 2 and 4% Mn. Since this small amount of Mn has no significant effect on the ZnO structure, no calculations on the cyclic cluster of cubic MnO are presented here. However, Mn was parametrized to fit the structure and band gap of cubic MnO. The Mn atoms are located at the sites of the Zn atoms. This is energetically the most favorable situation. The formal oxidation number of Mn is 2. The most stable situation was reached for Mn atoms with a multiplicity of 6. This means that the two valence electrons in 4s orbitals with opposite spin are formally transferred to the adjacent oxygens and the remaining five valence electrons in 3d orbitals are oriented with parallel spin. In the case of two Mn atoms, the local spins of these atoms can be oriented antiparallel or parallel. The first case is a model for antiferromagnetism, the second for ferromagnetism. It should be mentioned that the present approach, based on an unrestricted Hartree−Fock (UHF) single determinant, is only an approximation for the case of Mn doping both to the antiferromagnetic $S = 0$ state, called the broken-symmetry (BS) state, and the high-spin (HS) ferromagnetic state. A detailed discussion can be found elsewhere.[43,44] However, this restriction is less severe in parametrized semiempirical methods than in ab initio or DFT methods.

TABLE 1: Influence of Mn Doping and Intrinsic Defects on the Band Gap E_g (eV) of ZnO for Various Multiplicities M Related to Antiferromagnetic (a) and Ferromagnetic (f) Spin States

cyclic cluster	M	state	defect	site	E_g
$Zn_{47}MnO_{48}$	6		Mn	Zn	2.37
$Zn_{46}Mn_2O_{48}$	1/11	a/f	2Mn	2Zn	2.33/2.35
$Zn_{47}MnO_{47}$	6		Mn, V_O	Zn, O	2.13
$Zn_{46}Mn_2O_{47}$	1/11	a/f	2Mn, V_O	2Zn, O	2.07/2.11
$Zn_{47}Mn_2O_{48}$	1/11	a/f	2Mn, Zn_i	2Zn, V_{Zn_i}	2.29/2.29
$Zn_{45}Mn_2O_{48}$	1/11	a/f	2Mn, V_{Zn}	2Zn, Zn	2.13/2.15

After full optimization of the cyclic cluster, there is, of course, local relaxation around the Mn atoms, which was taken into account. In the case of $Zn_{47}MnO_{48}$, the MnO intralayer distance was 1.833 Å. This means a substantial shortening compared to the respective ZnO distance of 1.951 Å in $Zn_{48}O_{48}$.[39] A much smaller change was found for the shortest MnZn distance (3.229 Å) compared to the ZnZn distance (3.216 Å) in $Zn_{48}O_{48}$. All possible relative geometrical arrangements of the two Mn atoms were studied. In all cases, it was found the antiferromagnetic spin state is more stable than the ferromagnetic spin state. A typical energy difference is 1 kJ/mol. The dependence of the energies of both spin states on the MnMn distance was negligible.

The results for the lowest band gaps are listed in Table 1. We observe that the band gap is substantially decreased to 2.37 eV for the substitution by one Mn atom. A density of states (DOS) plot of $Zn_{47}MnO_{48}$ is presented in Figure 1. It shows the distribution of molecular orbitals with α and β spin. We compare this plot with the DOS plots of $Zn_{48}O_{48}$ (defect-free ZnO) and $Zn_{48}O_{47}$ (ZnO with oxygen vacancy) discussed previously.[39] In that case, the creation of an oxygen vacancy formally removes four doubly occupied MOs related to the O^{2-} anion, but since the total system is neutral, i.e., only six electrons of the O atom are removed, the two additional electrons have to move to the LUMO of $Zn_{48}O_{48}$, which is dominated by zinc orbitals. This MO becomes the HOMO of $Zn_{48}O_{47}$. In the case of Zn by Mn substitution, Zn^{2+} is replaced by Mn^{2+}. From the 10 Zn 3d electrons in occupied orbitals, 5 are removed and the other 5 are replaced by Mn electrons in higher-lying orbitals. In this way, the former LUMO of $Zn_{48}O_{48}$ is occupied with one electron and is the α-HOMO of $Zn_{47}MnO_{48}$. The Zn character of the LUMO is now partially replaced by Mn character. A localized description is, however, not possible, since the MOs

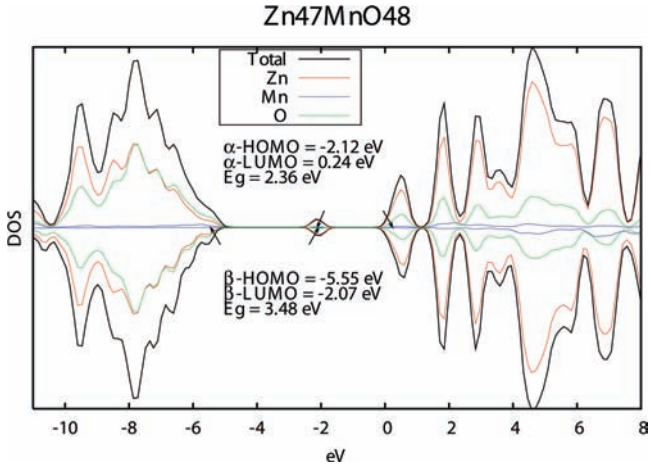

Figure 1. Density of states (DOS) curves and HOMO−LUMO gap E_g (eV) for cyclic cluster $Zn_{48}MnO_{47}$.

are delocalized. Here, the band gap is approximated by the energy difference of α-LUMO and α-HOMO. Mn substitution results in a substantial decrease of the band gap compared to $Zn_{48}O_{48}$. A small further decrease occurred for the second substitution. There is only a very small band gap difference between the antiferromagnetic and ferromagnetic spin arrangements. The decrease of the band gap was also observed in most recent experiments. It follows the same trend as the one predicted by our calculations, namely, that a 2% Mn substitution causes a substantial decrease, whereas another 2% substitution has a much smaller effect. A detailed discussion can be found in a combined experimental and theoretical study.[45]

The discrepancy to the previously mentioned experimental results of an increase of the band gap with increasing manganese content could be clarified. From the figures presented by Tiwari et al.,[13] it is apparent that these authors have ignored the low intensity absorbance due to partially forbidden transitions to which our calculations apply. The increase of the band gap found by experimental[5,13,16] and other theoretical[17] studies could possibly be related to the difference between β-LUMO and β-HOMO. Mn substitution increased this difference from 3.40 to 3.48 eV.

A further decrease of the band gap to 2.13 eV is achieved by the creation of a vacancy of an oxygen atom in addition to the substitution of a zinc atom by a manganese atom. A nearest neighbor distance of 1.95 Å between Mn and V_O was energetically most favorable. In previous work,[39] we have shown that an oxygen vacancy in the cyclic cluster $Zn_{48}O_{48}$ leads to a decrease of the band gap from 3.40 to 2.60 eV. A combination of Mn substitution and oxygen vacancy reinforces the decrease. There is a slight further decrease of the band gap upon the substitution of a second zinc atom by a manganese atom. Again, the antiferromagnetic spin orientation was found to be more favorable than the ferromagnetic spin orientation by less than 1 kJ/mol.

We have also studied the cases of a zinc interstitial Zn_i or a zinc vacancy V_{Zn} in combination with two Mn atoms. In both cases, the band gap is decreased regardless of the spin state. Whereas the antiferromagnetic and ferromagnetic arrangements differ in energy by less than 0.1 kJ/mol in the case of the zinc interstitial, the antiferromagnetic arrangement is more stable by a few kJ/mol for the case of the zinc vacancy.

An explicit discussion of substitution and defects based on DFT calculations was given by Iuşan et al.[17] In the case of pure Mn substitution and additional zinc interstitials or oxygen vacancies, the antiferromagnetic state was found to be favored. It was predicted that an increasing amount of Zn vacancies would eventually favor the ferromagnetic state. Our calculations were concerned with a small Zn vacancy concentration of only 2% compared to 8% in the DFT study.[17] Therefore, we cannot confirm nor contradict their prediction. Unfortunately, comparison of band gap trends between our calculations and these DFT calculations cannot be made, because the DFT calculations predict an unrealistically low band gap of 0.7 eV for ZnO.

TABLE 2: Influence of Fe Doping and Intrinsic Defects on the Band Gap E_g (eV) of ZnO for Various Multiplicities M Related to Antiferromagnetic (a) and Ferromagnetic (f) Spin States

cyclic cluster	M	state	defect	site	E_g
$Zn_{47}FeO_{48}$	5		Fe	Zn	3.24
$Zn_{46}Fe_2O_{48}$	1/9	a/f	2Fe	2Zn	3.12/3.03
$Zn_{47}FeO_{47}$	5		Fe, V_O	Zn, O	2.22
$Zn_{46}Fe_2O_{47}$	1/9	a/f	2Fe, V_O	2Zn, O	2.16/2.16
$Zn_{47}Fe_2O_{48}$	1/9	a/f	2Fe, Zn_i	2Zn, V_{Zn_i}	2.29/2.30
$Zn_{45}Fe_2O_{48}$	1/9	a/f	2Fe, V_{Zn}	2Zn, Zn	3.22/3.06

Some additional information can be gained by consideration of the spin density. There is a variety of population analyses which yield different results for atomic charges depending on the underlying method (ab initio, DFT, semiempirical), basis set, and type of analysis.[46] Such methods can only show trends. MSINDO is based on orthogonalized atomic orbitals (OAOs). The calculated spin density of Mn in cyclic $Zn_{47}MnO_{48}$ is 3.93 based on such OAOs, from which more than 95% is due to 3d orbitals. The spin density would be 5 in a Mn^{2+} cation. Since the total population of d orbitals is 4.5, i.e., close to 5, we can formally refer to Mn^{2+}, although there are also contributions of 4s and 4p.

3.2. Doping of ZnO with Fe. We found it now interesting to see whether the behavior of the electronic structure with respect to the band gap and relative stability of antiferromagnetic and ferromagnetic spin states would be similar in the case of doping zinc oxide with other transition metals. Chemical vapor transport allows a solution of 11 mol % FeO in ZnO.[42] We have substituted again one or two Zn atoms by Fe atoms in the cyclic cluster $Zn_{48}O_{48}$. In the case of doping with iron, the spin multiplicity of the reference Fe^{2+} ions in the favorable high spin case is 5 because there are formally five valence electrons with α spin and one valence electron with β spin in 3d orbitals. After full optimization of $Zn_{47}FeO_{48}$, it was found that the relaxation around the Fe atom is negligible with an FeO intralayer distance of 1.954 Å compared to the ZnO distance of 1.951 Å in $Zn_{48}O_{48}$. The same was found for the FeZn distance (3.212 Å) compared to the ZnZn distance (3.216 Å). For the case of two Fe atoms their spin orientation can be antiparallel or parallel giving again rise to antiferromagnetic and ferromagnetic situations.

The results for the band gaps are collected in Table 2. The DOS plot of $Zn_{47}FeO_{48}$ is presented in Figure 2. The even number of Fe^{2+} valence electrons and the partial pairing leads to very similar HOMOs and LUMOs for α and β spin. In contrast to the case of Mn doping, the effect of Fe doping on the band gap is rather insignificant. The DOS plot of $Zn_{47}FeO_{48}$ resembles that of $Zn_{48}O_{48}$ for the HOMO and LUMO. The small lowering of the band gap compared to $Zn_{48}O_{48}$ is due to the lowering of the LUMO. For one Fe atom in the cyclic cluster $Zn_{48}FeO_{48}$, the band gap lowering is 0.16 eV, and for two Fe atoms in $Zn_{48}Fe_2O_{48}$, there is another lowering of 0.12 eV for the antiferromagnetic state and 0.22 eV for the ferromagnetic state. For the case of an oxygen vacancy and a zinc interstitial, the band gap is influenced primarily by these defects. In

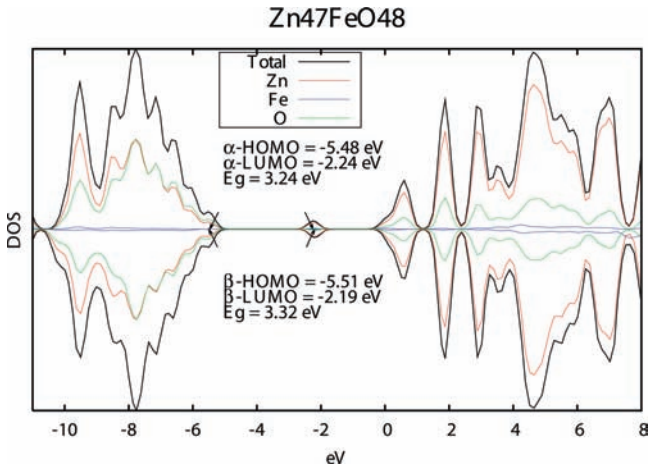

Figure 2. Density of states (DOS) curves and HOMO−LUMO gap E_g (eV) for cyclic cluster $Zn_{48}FeO_{47}$.

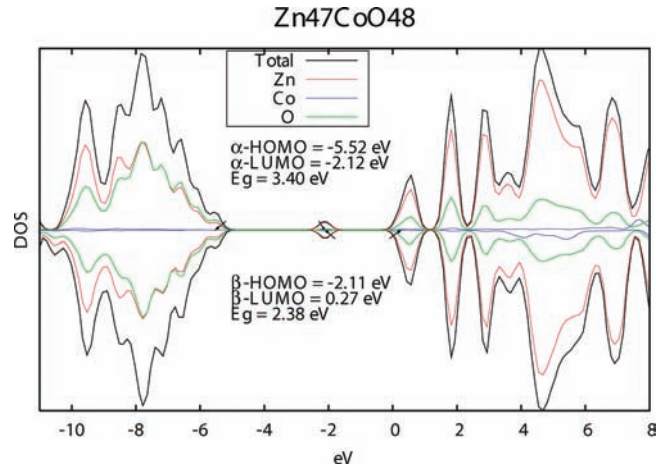

Figure 3. Density of states (DOS) curves and HOMO−LUMO gap E_g (eV) for cyclic cluster $Zn_{48}CoO_{47}$.

consequence, the lowering of the band gap is similar to the one caused by Mn doping. However, in the case of an additional zinc vacancy, the band gap lowering is small and similar to the one for pure zinc substitution by two Fe atoms.

In terms of stability, antiferromagnetic and ferromagnetic spin arrangements differ by less than 0.1 kJ/mol for pure Fe substitution and additional zinc vacancy or zinc interstitial. For an additional zinc vacancy, we found higher antiferromagnetic stability except for one case, where the Fe atoms were close to each other but had a large distance to the zinc vacancy.

The spin density of Fe in $Zn_{47}FeO_{48}$ was found to be 3.92, close to 4 of the Fe^{2+} cation. More than 98% is from 3d orbitals. The total d orbital population is 6.07. We can therefore refer to Fe^{2+}. From the spin densities, it became apparent that Fe^{2+} is present in all cases. Fe^{3+} cannot be found even in $Zn_{45}Fe_2O_{48}$.

3.3. Doping of ZnO with Co. Chemical vapor transport allows a solution of 5 mol % CoO in ZnO.[42] We have substituted one or two zinc atoms in the cyclic cluster $Zn_{48}O_{48}$ by Co atoms. In the case of Co doping, the formal spin multiplicity of the reference Co^{2+} ions is 4 due to five valence electrons with α spin and two valence electrons with β spin in 3d orbitals. For the case of a substitution of the Zn atom by one Co atom, the following results were obtained. The full optimization of the structure of $Zn_{47}CoO_{48}$ showed the intralayer CoO distance was shortened to 1.812 Å compared to the 1.951 Å of the ZnO distance in $Zn_{48}O_{48}$. Little change was found for the CoZn distance (3.226 Å) compared to the corresponding ZnZn distance (3.216 Å) in $Zn_{48}O_{48}$. Iuşan et al.[30] report a value of 1.98 Å for the intralayer CoO distances but no corresponding ZnO or CoZn distances. From the reported CoCo distances (3.24 Å), it is clear that the Zn framework is not substantially relaxed in agreement with our results. The DOS plot of $Zn_{47}CoO_{48}$ is presented in Figure 3. The plot is similar to the one of $Zn_{47}MnO_{48}$ except that the lower HOMO−LUMO gap is determined by the β orbitals. We observe that the band gap is substantially lowered by the substitution as in the case of Mn doping. Further defects such as oxygen vacancy, zinc interstitial, or zinc vacancy do not contribute to significant additional lowering which is again similar to the case of Mn doping (Table 3).

For the substitution by two Co atoms, we studied again cases with small and large CoCo distances. The antiferromagnetic spin arrangement was clearly favored by more than 2 kJ/mol. The Co atoms prefer the closest distance, but the energy differences to the other situations were less than 0.3 kJ/mol. This difference between the antiferromagnetic and ferromagnetic state was reduced to less than 0.1 kJ/mol for an additional oxygen vacancy or zinc interstitial. If an additional zinc vacancy was introduced, the ferromagnetic spin arrangement was found to be favored regardless of the relative distances between the two Co atoms and the vacancy.

The influence of cobalt clusters in ZnO was discussed by Iuşan et al.[29,30] With local spin density approximation (LSDA)+U calculations, they arrived at the conclusion that Co substitution in ZnO favors the antiferromagnetic state and Co clusters enhance its stability. This is qualitatively in line with our findings. Our results are also close to those by Ghopal and Spaldin[25] where a comparative study of Mn, Fe, and Co doping of ZnO was made via local spin density (LSDA) calculations but without additional defects. These authors conclude that Fe- or Co-doped ZnO is a more likely candidate for ferromagnetism than Mn-doped ZnO. In the latter case, clearly antiferromagnetism was predicted in agreement with our combined experimental and theoretical study.[45]

Our spin density calculations arrive at 3.64 for Co in $Zn_{47}CoO_{48}$ from which about 99% is due to 3d orbitals. The total 3d population is 6.35. We can still formally refer to Co^{2+}, where the spin density would be 3, because a lesser 3d population and some 4s and 4p populations in MO calculations based on OAOs are quite common. Spaldin[24] and Iuşan et al.[30] appear to arrive at a spin density of 3.0 in their LSDA calculation.

3.4. Mixed Doping of ZnO with Mn, Fe, and Co. In the case of mixed doping with Mn, Fe, and Co, the antiparallel spin orientation of pairs of different atoms in the cyclic cluster cannot lead to spin states of multiplicity 1. We call these states ferrimagnetic. The case of parallel orientation of spins of different doping atoms is called again ferromagnetic. Cases of small and large distances between the two doping atoms were studied. Here, the band gap is dominated by the atom which causes the largest lowering. This means that combination of Mn and Fe is dominated by Mn doping and the one of Co and Fe by Co doping. For mixed Mn and Co doping, we find a small further decrease of the band gap compared to the doping with either Mn or Co (Table 4).

In the case of mixed Mn and Co doping, we found that the ferromagnetic spin arrangement is favored by more than 2 kJ/mol over the ferrimagnetic arrangement. For the mixed Mn and Fe doping, the energy difference is only about 0.2 kJ/mol but still favoring the ferromagnetic state. In the case of mixed Fe and Co doping, the energy differences are about 0.1 kJ/mol in

TABLE 3: Influence of Co Doping and Intrinsic Defects on the Band Gap E_g (eV) of ZnO for Various Multiplicities M Related to Antiferromagnetic (a) and Ferromagnetic (f) Spin States

cyclic cluster	M	state	defect	site	E_g
$Zn_{47}CoO_{48}$	4		Co	Zn	2.38
$Zn_{46}Co_2O_{48}$	1/7	a/f	2Co	2Zn	2.40/2.37
$Zn_{47}CoO_{47}$	4		Co, V_O	Zn, O	2.28
$Zn_{46}Co_2O_{47}$	1/7	a/f	2Co, V_O	2Zn, O	2.30/2.28
$Zn_{47}Co_2O_{48}$	1/7	a/f	2Co, Zn_i	2Zn, V_{Zn_i}	2.21/2.19
$Zn_{45}Co_2O_{48}$	1/7	a/f	2Co, V_{Zn}	2Zn, Zn	2.20/2.26

TABLE 4: Influence of Mixed Mn, Fe, and Co Doping on the Band Gap E_g (eV) of ZnO for Various Multiplicities M Related to Ferrimagnetic (i) and Ferromagnetic (f) Spin States

cyclic cluster	M	state	defect	site	E_g
$Zn_{46}MnFeO_{48}$	2/10	i/f	Mn, Fe	2Zn	2.18/2.21
$Zn_{46}MnCoO_{48}$	3/9	i/f	Mn, Co	2Zn	2.04/2.34
$Zn_{46}FeCoO_{48}$	2/8	i/f	Fe, Co	2Zn	2.31/2.27

favor of the ferrimagnetic state. The qualitative results hold independently of the distances between the doping atoms.

4. Conclusion

Our investigation of the effect of doping of ZnO with Mn, Fe, and Co showed a pronounced effect on the band gap for Mn and Co, whereas the Fe substitution has only a minor effect. The lowering of the band gap in the case of Mn substitution is in line with recent experiments. The discrepancy to previous experimental work could be clarified. An additional oxygen vacancy or zinc interstitial can reduce the band gap substantially for Fe-doped ZnO, whereas only a slight further decrease was found for Mn- and Co-doped ZnO. This can be explained by the observation that the main effect is already found for the first Mn or Co substitution but not for the Fe substitution. Further substitution of introduction or defects can only be effective in the latter case. A zinc interstitial did not substantially change the band gap compared with the pure doping.

The modeling of antiferromagnetic, ferrimagnetic, and ferromagnetic spin arrangements by the substitution of two zinc atoms by two transition metal atoms resulted in the prediction that the antiferromagnetic arrangement is always more stable than the ferromagnetic arrangement. Additional insertion of oxygen vacancy or zinc interstitial can only reduce this difference for the first two defects. With an additional zinc vacancy, the parallel spin arrangement was always favored for doping with Co atoms and also in one case for doping with Fe atoms. This trend is in agreement with predictions from other authors. In the case of mixed Mn and Co substitution, the ferromagnetic arrangement was clearly favored over the ferrimagnetic arrangement, and in Mn and Fe doping, it was slightly favored.

Since chemical transport preparation of Mn-doped ZnO gave no indication of ferromagnetism, we suspect that the method of preparation may have an influence on the magnetic properties in the way that oxide grains of the doping transition metal or other more complicated defects could be responsible for the observed ferromagnetism. It seems more likely that Fe- or Co-doped ZnO can show ferromagetism, if particular defects are present or if they appear mixed with elements of lower spin multiplicity.

Acknowledgment. This work was partially supported by Deutsche Forschungsgemeinschaft. We thank Prof. M. Binnewies and Prof. K. D. Becker for helpful discussions.

References and Notes

(1) Hofmann, D. M. *Phys. Z.* **1999**, *30*, 69.
(2) Dietl, T.; Ohno, H.; Matsukura, F.; Cibert, J.; Ferrand, D. *Science* **2000**, *287*, 1019.
(3) Ohtomo, A.; Kawasaki, M.; Koida, T.; Masubuchi, K.; Koinuma, H.; Sakurai, Y.; Yoshida, Y.; Yasuda, T.; Segawa, Y. *Appl. Phys. Lett.* **1998**, *72*, 2466.
(4) Özgür, Ü.; Alivov, Ya, I.; Liu, C.; Teke, A.; Reshchikov, M. A.; Dogan, S.; Avrutin, V.; Cho, S.-J.; Morkoc, H. *J. Appl. Phys.* **2005**, *98*, 041301.
(5) Fukumura, T.; Zhengwu, J.; Ohtoma, A.; Koinuma, H.; Kawasaki, M. *Appl. Phys. Lett.* **1999**, *75*, 3366.
(6) Sharma, P.; Gupta, A.; Rao, K. V.; Owens, F. J.; Sharma, R.; Ahuja, R.; Guillen, J. M. O.; Johansson, B.; Gehring, G. A. *Nat. Mater.* **2003**, *2*, 673.
(7) Kunisu, M.; Oba, F.; Ikeno, H.; Tanaka, I.; Yamamoto, T. *Appl. Phys. Lett.* **2005**, *86*, 121902.
(8) Zhang, J.; Skomski, R.; Sellmeyer, D. J. *J. Appl. Phys.* **2005**, *97*, 10D303.
(9) Xu, Q.; Zhou, Y.; Zhang, X.; Chen, D.; Xie, Y.; Liu, T.; Yan, W. *Solid State Commun.* **2007**, *141*, 374.
(10) Xu, W.; Schmidt, H.; Hartmann, L.; Hochhuth, H.; Lorenz, M.; Setzer, A.; Esquinazi, P.; Meinecke, C.; Grundmann, M. *Appl. Phys. Lett.* **2007**, *91*, 092503.
(11) Céspedes, E.; Castro, G. R.; Jiménez-Villacorta, F.; de Andrés, A. *J. Phys.: Condens. Matter* **2008**, *20*, 095207.
(12) Bondino, F.; Garg, K. B.; Magnano, E.; Carleschi, E.; Heinonen, M.; Singhal, R. K.; Gaur, S. K.; Parmigiani, F. *J. Phys.: Condens. Matter* **2008**, *20*, 275205.
(13) Tiwari, A.; Jin, C.; Kvit, A.; Kumar, D.; Muthi, J. F.; Narayan, J. *Solid State Commun.* **2002**, *121*, 371.
(14) Kolesnik, S.; Dabrowski, B.; Mais, J. *J. Appl. Phys.* **2004**, *95*, 2582.
(15) Kolesnik, S.; Dabrowski, B. *J. Appl. Phys.* **2004**, *96*, 5379.
(16) Chikoidze, E.; Dumont, Y.; Jomard, F.; Ballutaud, D.; Galtier, P.; Gorochov, O. *J. Appl. Phys.* **2005**, *97*, 10D327.
(17) Iuşan, D.; Sanyal, B.; Eriksson, O. *Phys. Rev. B* **2006**, *74*, 235208.
(18) Rosa, A. L.; Ahuja, R. *J. Phys.: Condens. Matter* **2007**, *7*, 386232.
(19) Tuomisto, F.; Mycielski, A.; Grasza, K. *Superlattices Microstruct.* **2007**, *42*, 218.
(20) Mukadam, M. D.; Yusuf, S. M. *Physica B* **2008**, *403*, 2602.
(21) Risbud, A.; Spaldin, N. A.; Chen, Z. Q.; Stemmer, S.; Seshadri, R. *Phys. Rev. B* **2003**, *68*, 205202.
(22) Ueda, K.; Tabata, H.; Kawai, T. *Appl. Phys. Lett.* **2001**, *79*, 988.
(23) Kim, J. H.; Kim, H.; Ihm, Y. E.; Choo, W. K. *Physica B* **2003**, *327*, 304.
(24) Spaldin, N. A. *Phys. Rev. B* **2004**, *69*, 125201.
(25) Ghopal, P.; Spaldin, N. A. *Phys. Rev. B* **2006**, *74*, 094418.
(26) Lin, Y.; Jiang, D.; Lin, F.; Shi, W.; Ma, X. *J. Alloys Compd.* **2007**, *436*, 30.
(27) Mandal, S. K.; Nath, T. K.; Karmakar, D. *Philos. Mag.* **2008**, *8*, 365.
(28) Sun, Z.; Yan, W.; Zhang, G.; Oyanagi, H.; Wu, Z.; Liu, Q.; Wu, W.; Shi, T.; Pan, Z.; Xu, P.; Wei, S. *Phys. Rev. B* **2008**, *77*, 245208.
(29) Sanyal, B.; Knut, R.; Grånäs, O.; Iuşan, D. M.; Karis, O.; Eriksson, O. *J. Appl. Phys.* **2008**, *103*, 07D131.
(30) Iuşan, D. M.; Kabir, M.; Grånäs, O.; Eriksson, O.; Sanyal, B. *Phys. Rev. B* **2009**, *79*, 125202.
(31) Ahlswede, B.; Jug, K. *J. Comput. Chem.* **1999**, *20*, 563.
(32) Ahlswede, B.; Jug, K. *J. Comput. Chem.* **1999**, *20*, 572.
(33) Bredow, T.; Geudtner, G.; Jug, K. *J. Comput. Chem.* **2001**, *22*, 861.
(34) Bredow, T.; Geudtner, G.; Jug, K. *J. Comput. Chem.* **2001**, *22*, 89.
(35) Janetzko, F.; Bredow, T.; Jug, K. *J. Chem. Phys.* **2002**, *116*, 8994.
(36) Jug, K.; Geudtner, G. *Chem. Phys. Lett.* **1993**, *54*, 1948.
(37) Huzinaga, S. *J. Chem. Phys.* **1971**, *116*, 8994.
(38) Janetzko, F.; Jug, K. *J. Phys. Chem. A* **2004**, *108*, 5449.
(39) Jug, K.; Tikhomirov, V. A. *J. Comput. Chem.* **2008**, *29*, 2250.
(40) Lide, D. R. *Handbook of Chemistry and Physics*, 79th ed.; CRC Press: Boca Raton, FL, 1998/1999.
(41) Hümmer, K. *Phys. Status Solidi B* **1973**, *56*, 249.
(42) Locmelis, S.; Binnewies, M. *Z. Anorg. Allg. Chem.* **1999**, *625*, 1573.
(43) Nair, N. N.; Schreiner, E.; Pollet, R.; Staemmler, V.; Marx, D. *J. Chem. Theory Comput.* **2008**, *4*, 1174.
(44) Neese, F. *J. Phys. Chem. Solids* **2004**, *65*, 781.
(45) Saal, H.; Binnewies, M.; Schrader, M.; Börger, A.; Becker, K. D.; Tikhomirov, V. A.; Jug, K. *Chem. Eur. J.* **2009**, *15*, 6408.
(46) Jug, K.; Maksić, Z. B. In *Theoretical Models of Chemical Bonding*; Maksić, Z. B., Ed.; Springer: Heidelberg, Germany, 1991; Part 3, p 235.

JP902532A